

1 **Characterization of organic nitrogen in aerosols at a forest site in** 2 **the southern Appalachian Mountains**

3
4 Xi Chen¹, Mingjie Xie^{2,a}, Michael D. Hays¹, Eric Edgerton³, Donna Schwede⁴, John T. Walker^{1,*}

5 ¹National Risk Management Research Laboratory, Office of Research and Development, U.S.
6 Environmental Protection Agency, Research Triangle Park, North Carolina, 27711, U.S.A.

7
8 ²Oak Ridge Institute for Science and Education (ORISE), National Risk Management Research
9 Laboratory, Office of Research and Development, U.S. Environmental Protection Agency,
10 Research Triangle Park, North Carolina, 27711, U.S.A.

11
12 ³Atmospheric Research and Analysis, Inc., Cary, NC, 27513

13
14 ⁴National Exposure Research Laboratory, Office of Research and Development, U.S.
15 Environmental Protection Agency, Research Triangle Park, North Carolina, 27711, U.S.A.

16
17 ^aPresent address: School of Environmental Science and Engineering, Nanjing University of
18 Information Science & Technology, Nanjing 210044, China

19
20
21 *Corresponding Author: Tel.: +1 919 541 2288. Email: Walker.JohnT@epa.gov.

22 23 **Abstract**

24 This study investigates the composition of organic particulate matter in PM_{2.5} in a remote
25 montane forest in the southeastern U.S., focusing on the role of organic nitrogen (N) in sulfur-
26 containing secondary organic aerosol (nitrooxy-organosulfates) and aerosols associated with
27 biomass burning (nitro-aromatics). Bulk water soluble organic N (WSON) represented ~ 14%
28 w/w of water soluble total N (WSTN) in PM_{2.5}, on average, across seasonal measurement
29 campaigns conducted in the spring, summer, and fall of 2015. Largest contributions of WSON to
30 WSTN were observed in spring (~ 18% w/w) and lowest in the fall (~10% w/w). On average,
31 identified nitro-aromatic and nitrooxy-organosulfate compounds accounted for a small fraction
32 of WSON, ranging from ~ 1% in spring to ~ 4% in fall, though were observed to contribute as
33 much as 28% w/w of WSON in individual samples which were impacted by local biomass
34 burning. Highest concentrations of oxidized organic N species occurred during summer (average
35 of 0.65ngN/m³) along with a greater relative abundance of higher generation oxygenated

36 terpenoic acids, indicating an association with more aged aerosol. Highest concentrations of
37 nitro-aromatics (eg. nitrocatechol and methyl-nitrocatechol), levoglucosan, and aged SOA tracers
38 were observed during fall, associated with aged biomass burning plumes. Nighttime nitrate
39 radical chemistry is the most likely formation pathway for nitrooxy-organosulfates observed at
40 this low NO_x site (generally <1ppb). Isoprene derived organosulfate (MW216, 2-methyltetrol
41 derived), which is formed from isoprene epoxydiols (IEPOX) under low NO_x conditions, was
42 the most abundant individual organosulfate. Concentration weighted average WSON/WSOC
43 ratios for nitro-aromatics + organosulfates + terpenoic acids were one order of magnitude lower
44 than the overall aerosol WSON/WSOC ratio, indicating the presence of other uncharacterized
45 higher N content species. Although nitrooxy-organosulfates and nitro-aromatics contributed a
46 small fraction of WSON, our results provide new insight into the atmospheric formation
47 processes and sources of these largely uncharacterized components of atmospheric organic N,
48 which also helps to advance the atmospheric models to better understand the chemistry and
49 deposition of reactive N.

50

51 **1. Introduction**

52

53 There is extensive evidence showing that boreal and temperate forests are affected by
54 anthropogenic activities, both industrial and agricultural. Such activity results in unprecedented
55 quantities of reactive nitrogen (N) being released into the atmosphere, subsequently altering
56 global nitrogen and carbon (C) biogeochemical cycles (Bragazza et al., 2006; Doney et al., 2007;
57 Ollinger et al., 2002; Magnani et al., 2007; Neff et al., 2002a,b; Pregitzer et al., 2008). Nitrogen
58 enters natural ecosystems through atmospheric deposition and biological fixation, and is mainly
59 lost through leaching and gaseous fluxes back to the atmosphere (Hungate et al., 2003).

60 Atmospheric deposition of N to terrestrial ecosystems may lead to soil and aquatic acidification,
61 nutrient imbalance and enrichment, plant damage and microbial community changes as well as
62 loss of biodiversity (Bobbink et al., 1998; Magnani et al., 2007; Lohse et al, 2008; Simkin et al.,
63 2016).

64 In the United States, deposition of atmospheric pollutants including N is monitored by
65 the National Atmospheric Deposition Program (NADP) and EPA's Clean Air Status and Trends
66 Network (CASNET). However, these networks focus only on inorganic N species (eg.
67 NH₃/NH₄⁺ and HNO₃/NO₃⁻). Recent studies shed light on the importance of organic N

68 deposition, which is not routinely measured in national networks. On a global basis, organic N
69 may contribute ~ 25 percent of the total N deposition (Gonzalez Benitez et al., 2009; Jickells et
70 al., 2013; Kanakidou et al., 2012; Keene et al., 2002; Neff et al., 2002a; Zhang et al., 2012).
71 Although ubiquitous, widespread routine monitoring of organic N in the atmosphere is inhibited
72 due to difficulties in sampling (Walker et al., 2012) and inability to fully speciate the wide range
73 of constituents that make up this large pool of atmospheric N (Altieri et al., 2009, 2012; Cape et
74 al., 2011; Neff et al., 2002a; Samy et al., 2013). For these reasons, understanding of the sources,
75 atmospheric chemistry, and deposition of organic nitrogen remains limited.

76 Atmospheric N from biogenic and anthropogenic emissions sources undergoes complex
77 transformation processes and photochemical reactions. Consequently, apportionment of
78 atmospheric organic N to potential sources is challenging. However, such information is required
79 to advance atmospheric N models applied to better understand the global N cycle. For example,
80 Miyazaki et al. (2014) examined aerosols collected in a deciduous forest and found in the
81 summer that water soluble organic N (WSO_N) correlated positively to biogenic hydrocarbon
82 oxidation; and during fall WSO_N in the coarse particle fraction was associated with primary
83 biological emissions (e.g. emitted from soil, vegetation, pollen and bacteria). Such patterns
84 underscore that atmospheric organic N measured in forested landscapes originates from a variety
85 of sources that contribute differently across seasons.

86 Recent advancements have been made in speciation of organic N in aerosol for some
87 groups of compounds including amines, amino acids and other nitrogenated functional groups
88 such as organonitrates (Day et al., 2010; Place et al., 2017; Samy et al., 2013). Organic N in
89 secondary aerosol and aerosols associated with biomass burning sources are areas of increasing
90 interest, from both atmospheric chemistry and ecosystem exposure perspectives, where more
91 information is needed. Studies of secondary organic aerosols (SOA) have identified a variety of
92 nitrated organosulfate compounds (e.g. nitrooxy-organosulfates) in both chamber and ambient
93 aerosol samples following isoprene and monoterpenes oxidation. These compounds are either
94 produced under high NO_x conditions or from nighttime NO₃ radical chemistry (Surratt et al.,
95 2006, 2007, 2008, 2010; Darer et al., 2011; Lin et al., 2013a; He et al., 2014; Worton et al.,
96 2013). Potential SOA precursors such as unsaturated green leaf volatiles (GLVs) released by
97 wounded plants (e.g. crop harvesting and insect attacks) may contribute substantially to the
98 budget of biogenic SOA formation especially in remote forests (Gomez-Gonzalez et al., 2008;

99 Hamilton et al., 2013; Shalamzari et al., 2016). The detection of reaction products such as
100 organosulfates and nitrooxy-organosulfates in ambient aerosols provides strong evidence of
101 influence from anthropogenic sources (e.g. SO₂ and NO_x) interacting with biogenic precursors to
102 form nitrogenated SOA (Chan et al., 2010; Lin et al., 2013a; Meade et al., 2016).

103 In addition to being present in sulfur-containing SOA, organic nitrogen, specifically
104 nitro-aromatic compounds (e.g. nitrophenols and nitrocatechols), have been characterized as
105 chemical tracers from biomass burning (e.g. wildland and prescribed smoke, bushfires,
106 residential wood burning). This is in addition to levoglucosan, a widely used tracer of biomass
107 burning (Iinuma et al., 2010, 2016; Kahnt et al., 2013; Kitanovski et al., 2012; Gaston et al.,
108 2016). These nitrated compounds can form during pyrolysis of plant biopolymers such as
109 cellulose. Furthermore, as combustion byproducts, these compounds are often defined as brown
110 carbon (BrC) and thus potentially light absorbing (Mohr et al., 2013; Liu et al., 2015).
111 Presumably, nitro-aromatics could constitute a substantial portion of atmospheric organic N in
112 aerosols collected in regions affected by biomass burning.

113 This study investigates the composition of organic particulate matter in a remote montane
114 forest in the southeastern U.S., focusing on the role of organic N in sulfur-containing SOA and
115 aerosols associated with biomass burning. Measurements target four groups of compounds: 1)
116 nitro-aromatics associated with biomass burning; 2) organosulfates and nitrooxy-organosulfates
117 produced from biogenic SOA precursors (i.e., isoprene, monoterpenes and unsaturated
118 aldehydes) interacting with anthropogenic pollutants; 3) terpenoic acids formed from
119 monoterpene oxidation; and 4) organic molecular markers including methyltetrols, C-5 alkene
120 triols, 2-methylglyceric acid, 3-hydroxyglutaric acid and levoglucosan. Terpenoic acids and
121 organic markers are included to assist in characterizing the extent of biogenic compound
122 oxidation and atmospheric processing (i.e., aerosol aging) as well as contributions from biomass
123 burning sources. Aerosol bulk chemical measurements are conducted to estimate total water
124 soluble organic N and C concentrations. Characterization of seasonal patterns in concentrations
125 of organic N species and assessment of potential sources and formation processes are
126 emphasized.

127

128 **2. Experimental methods and materials**

129 **2.1 Sampling site and atmospheric aerosol collection**

130 The study was conducted at the U.S. Forest Service Coweeta Hydrologic Laboratory, a
131 2185-ha experimental forest in southwestern, North Carolina, USA (35°3' N, 83°25' W) near the
132 southern end of the Appalachian Mountain chain. The climate is classified as maritime, humid
133 temperate, with mean monthly temperatures ranging from 3.3°C in January to 21.6°C in July
134 (Swift et al., 1988). Elevation ranges from 675 to 1592 m with a corresponding range in annual
135 precipitation of 1800 to 2500 mm (Swank and Crossley, 1988). The vegetation is characterized
136 as mixed coniferous/deciduous including oak, pines, and hardwoods (Bolstad et al, 1998).
137 Atmospheric measurements were conducted in the lowest part of the basin (686 m), collocated
138 with long term measurements of air and precipitation chemistry conducted by CASTNET and
139 NADP networks, respectively.

140 The sampling site is 5 km west of Otto, NC (population 2500) and Highway 23 (Figure
141 S1, supplemental material). Land to the north, west and south of Coweeta is undeveloped forest.
142 Typical rural development is present to the east of the site, consisting of houses and small scale
143 farming for hay and crop production including some scattered cow and horse pastures, which are
144 small local ammonia (NH₃) emission sources. The nearest metropolitan areas include Atlanta,
145 Georgia (175 km southwest), Chattanooga, Tennessee (175 km west), Knoxville, Tennessee (110
146 km north/northwest), Asheville, North Carolina (100 km northeast), and Greeneville, South
147 Carolina (100 km southeast). The location of the sampling site within the context of NO_x and
148 SO₂ point sources in the eastern U.S. is shown in supplemental material (Figure S2). Only minor
149 point sources are present within ~ 100 km of the site.

150 The study period summarized here comprises three seasonal intensives conducted during
151 the spring, summer and fall of 2015. Each campaign was conducted for approximately 3 weeks
152 (21 May to 9 June, 6 August to 25 August, 9 October to 26 October). A high-volume Tisch TE-
153 1000 (Tisch Environmental, Cleves, OH) dual cyclone PM_{2.5} sampler operated at a flow rate of
154 230 L/min was set up on the ground to collect 24 hr (started at 7am local time) integrated
155 samples on pre-baked (550°C for 12hrs) quartz fiber (QF) filters (90mm, Pall Corporation, Port
156 Washington, NY). Under some conditions, the 24hr integrated filter sampling technique may not
157 fully retain all semi-volatile organic nitrogen compounds (Gonzalez Benitez et al., 2009). Field
158 blanks were collected the same way except being loaded in the sampler without the pump
159 switched on. A total of 58 ambient samples and 10 field blanks were obtained. Collected filter

160 samples were transferred back to the laboratory in a cooler and stored in a freezer at -20 °C
161 before chemical analysis.

162 2.2 Trace gas and meteorological measurements

163 During the spring 2015 campaign, NO_x concentrations were measured on a short tower
164 (7 m above ground) co-located with the CASTNET and high volume PM samplers. NO_x
165 concentrations were measured using a commercial NO-NO₂-NO_x analyzer (model 42S, Thermo
166 Environmental Instruments, Incorporated, Franklin, MA). Briefly, nitric oxide (NO) is measured
167 directly on one channel by chemiluminescence. On a 2nd channel, NO₂ is converted to NO by a
168 molybdenum catalyst heated to 325°C, yielding the concentration of NO_x (NO + NO₂). This
169 approach may overestimate NO_x since other oxidized nitrogen gases such as HNO₃, PAN and
170 HONO could also be reduced to NO on the heated molybdenum surface (Fehsenfeld et al., 1987;
171 Williams et al., 1998; Zellweger et al., 2000). However, the use of an inlet filter and
172 approximately 12 m of sample line between the atmospheric inlet and converter likely minimized
173 the potential bias from HNO₃. For subsequent campaigns, NO_x concentrations were estimated
174 from a co-located NO_y analyzer. Similar to the NO_x instrument, NO_y and HNO₃ were also
175 measured using a modified model 42S NO-NO₂-NO_x analyzer. The NO_y technique is described
176 in detail by Williams et al. (1998). Briefly, total oxidized reactive nitrogen (NO_y) is converted to
177 NO using a molybdenum catalyst heated to 325°C. On a 2nd channel, a metal denuder coated with
178 potassium chloride (KCl) is used to remove HNO₃ before passing through a 2nd molybdenum
179 converter heated to 325°C. The difference between the total NO_y measurement and the HNO₃-
180 scrubbed NO_y measurement is interpreted as HNO₃. NO_x concentrations were estimated from
181 the differences between measured NO_y and HNO₃, which provided an upper bound estimation as
182 gaseous N containing species were not excluded (eg. PAN and organic nitrates). Hourly ozone
183 concentrations were measured by CASTNET (U.S. EPA, 2017) on a co-located 10m tower.
184 Hourly meteorological data were provided by CASTNET (U.S. EPA, 2017) and Forest Service
185 (Miniat et al 2015; Oishi et al., 2017), including temperature, relative humidity, solar radiation
186 and precipitation.

187

188 2.3 Chemical analysis

189 2.3.1 Elemental and organic carbon analysis

190 A 1.5cm² QF punch was analyzed for elemental carbon (EC) and organic carbon (OC) using
191 a thermo-optical transmittance (TOT) method (Sunset Laboratory Inc, Oregon, USA) (Birch and
192 Cary, 1996).

193 2.3.2 Water soluble species by Ion Chromatography (IC) and Total Organic Carbon/Total 194 Nitrogen (TOC/TN) analyzers

195 A second QF punch (1.5cm²) from each sample was extracted with DI water (18.2
196 MΩ·cm, Milli-Q Reference system, Millipore, Burlington, MA) in an ultrasonic bath for 45 min.
197 The sample extract was filtered through a 0.2μm pore size PTFE membrane syringe filter (Iso-
198 disc, Sigma Aldrich, St. Louis, MO) before subsequent analyses.

199 Water soluble organic carbon (WSOC) and total N (WSTN) concentrations were
200 measured using a chemiluminescence method that included a total organic carbon analyzer
201 (TOC-Vcsh) combined with a total nitrogen module (TNM-1) (Shimadzu Scientific Instruments,
202 Columbia, MD). For WSOC measurements, 25% phosphoric acid was mixed with sample
203 extract (resulting in a 1.5% acid mixture) and sparged for 3 min to remove any existing
204 carbonate/bicarbonate.

205 Inorganic species (NH₄⁺, NO₃⁻, NO₂⁻ and SO₄²⁻) were analyzed using ion chromatography
206 (IC, Dionex model ICS-2100, Thermo Scientific, Waltham, MA). The IC was equipped with
207 guard (IonPac 2mm AG23) and analytical columns (AS23) for anions. The samples were
208 analyzed using an isocratic eluent mix carbonate/bicarbonate (4.5/0.8mM) at a flow rate of 0.25
209 mL/min. Cations were analyzed by Dionex IonPac 2mm CG12 guard and CS12 analytical
210 columns; separations were conducted using 20mM methanesulfonic acid (MSA) as eluent at a
211 flow rate of 0.25mL/min. Multi-point (≥5) calibration was conducted using a mixture prepared
212 from individual inorganic standards (Inorganic Ventures, Christiansburg, VA). A mid-level
213 accuracy check standard was prepared from certified standards mix (AccuStandard, New Haven,
214 CT) for quality assurance/quality control purposes.

215

216 2.3.3 UV-Vis light absorption analysis

217 Several studies have shown that methanol can extract aerosol OC at higher efficiencies
218 than water, and that a large fraction of light absorption in the near-UV and visible ranges is
219 ascribed to water insoluble OC (Chen and Bond, 2010; Liu et al., 2013; Cheng et al., 2016). In
220 this study, a QF punch (1.5 cm²) was extracted with 5 mL methanol (HPLC grade, Thermo

221 Fisher Scientific Inc.) in a tightly closed amber vial, sonicated for 15 min, and then filtered
222 through a 0.2 μm pore size PTFE filter (Iso-disc, Sigma Aldrich, St. Louis, MO). The light
223 absorption of filtered extracts was measured with a UV-Vis spectrometer over $\lambda = 200\text{-}900\text{ nm}$ at
224 0.2 nm resolution (V660, Jasco Incorporated, Easton MD). The wavelength accuracy is better
225 than $\pm 0.3\text{ nm}$; the wavelength repeatability is less than $\pm 0.05\text{ nm}$. A reference cuvette
226 containing methanol was used to account for solvent absorption. The UV-Vis absorption of field
227 blank samples was negligible compared to ambient samples, but used for correction nonetheless.
228 For ease of analysis, the absorption at 365 nm referencing to absorption at 700 nm was used as a
229 general measure of the absorption by all aerosol chromophore components (Hecobian et al.,
230 2010).

231

232 2.3.4. Analysis of isoprene and monoterpene SOA markers and anhydrosugars by GC-MS

233 Aliquots of each filter (roughly $\frac{1}{4}$) were extracted by 10 mL of methanol and methylene
234 chloride mixture (1:1, v/v) ultrasonically twice (15 minutes each). The total extract was filtered
235 and concentrated to a final volume of $\sim 0.5\text{ mL}$. Next, extracts were transferred to a 2 mL glass
236 vial and concentrated to dryness under a gentle stream of ultrapure N_2 and reacted with 50 μL of
237 N, O-bis(trimethylsilyl)trifluoroacetamide (BSTFA) containing 1% trimethylchlorosilane
238 (TMCS) and 10 μL of pyridine for 3 h at 70 $^\circ\text{C}$. After cooling down to room temperature,
239 internal standards (mixture of 17.6 $\text{ng } \mu\text{L}^{-1}$ acenaphthalene-d10 and 18.6 $\text{ng } \mu\text{L}^{-1}$ pyrene-d4
240 mixed in hexane) and pure hexane were added. The resulting solution was analyzed by an
241 Agilent 6890N gas chromatograph (GC) coupled with an Agilent 5975 mass spectrometer (MS)
242 operated in the electron ionization mode (70 eV). An aliquot of 2 μL of each sample was injected
243 in splitless mode. The GC separation was carried out on a DB-5 ms capillary column (30 m \times
244 0.25 mm \times 0.25 μm , Agilent Technologies, Santa Clara, CA). The GC oven temperature was
245 programmed from 50 $^\circ\text{C}$ (hold for 2 min) to 120 $^\circ\text{C}$ at 30 $^\circ\text{C min}^{-1}$ then ramped at 6 $^\circ\text{C min}^{-1}$ to
246 a final temperature of 300 $^\circ\text{C}$ (hold for 10 min). Linear calibration curves were derived from six
247 dilutions of quantification standards. Anhydrosugars (levoglucosan) were quantified using
248 authentic standard; 2-methyltetrols (2-methylthreitol and 2-methylerythritol) and C-5 alkene
249 triols were quantified using meso-erythritol; other SOA tracers (e.g., hydroxyl dicarboxylic acid)
250 were quantified using cis-ketopinic acid (KPA) (refer to supplemental information Table S1).
251 The species not quantified using authentic standards were identified by the comparison of mass

252 spectra to previously reported data (Claeys, et al., 2004, 2007; Surratt et al., 2006; Kleindienst et
253 al., 2007). Field blanks were collected and no contamination was observed for identified species.

254

255 2.3.5. Analysis of organosulfates, terpenoic acids and nitro-aromatics by High Performance
256 Liquid Chromatography- electrospray ionization-Quadrupole time-of-flight-Mass
257 Spectrometer (HPLC-ESI(-)-QTOF-MS)

258 Approximately 3-5 mL of methanol was used to ultrasonically extract (twice for 15 min)
259 roughly half of each 90mm QF sample. Internal standards (I.S.) were spiked onto each filter
260 sample prior to extraction (refer to Table S2, S3 and S4 for individual compounds and surrogate
261 standards used for each group of compounds). Extracts were filtered into a pear-shaped glass
262 flask (50 mL) and rotary evaporated to ~0.1 mL. The concentrated extracts were then transferred
263 into a 2 mL amber vial that was rinsed with methanol 2-3 times. The final sample extract volume
264 was ~500 μ L prior to analysis. All the glassware used during the extraction procedure was pre-
265 baked at 550°C overnight. Extracted samples were stored at or below -20 °C prior to analysis and
266 typically analyzed within 7 d.

267 An HPLC coupled with a quadrupole time-of-flight mass spectrometer (1200 series LC
268 and QTOF-MS, Model 6520, Agilent Technologies, Palo Alto, CA) was used for target
269 compound identification and quantification. The QTOF-MS instrument was equipped with a
270 multimode ion source operated in electrospray ionization (ESI) negative (-) mode. Optimal
271 conditions were achieved under parameters of 2000 V capillary voltage, 140 V fragmentor
272 voltage, 65 V skimmer voltage, 300 °C gas temperature, 5 L/min drying gas flow rate and 40
273 psig nebulizer. The ESI-QTOF-MS was operated over the m/z range of 40 to 1000 at a 3
274 spectra/s acquisition rate. Target compounds separation was achieved by a C18 column (2.1 \times 100
275 mm, 1.8 μ m particle size, Zorbax Eclipse Plus, Agilent Technologies) with an injection volume
276 of 2 μ L and flow rate of 0.2 mL/min. The column temperature was kept at 40 °C, and gradient
277 separation was conducted with 0.2% acetic acid (v:v) in water (eluent A) and methanol (eluent
278 B). The eluent B was maintained at 25% for the first 3 min, increased to 100% in 10 min, held at
279 100% from 10 to 32 min, and then dropped back to 25% from 32 to 37 min, with a 3 min post
280 run time. During each sample run, reference ions were continuously monitored to provide
281 accurate mass corrections (purine and HP-0921 acetate adduct, Agilent G1969-85001).
282 Typically, the instrument exhibited 2 ppm mass accuracy. Tandem MS was conducted by

283 targeting ions under collision-induced dissociation (CID) to determine parent ion structures.
284 Agilent software Mass hunter was used for data acquisition (Version B05) and for further data
285 analysis (Qualitative and Quantitative Analysis, Version B07). The mass accuracy for compound
286 identification and quantification was set at ± 10 ppm. Calibration curves were generated from
287 diluted standard compound mixtures. Recoveries of the extraction and quantification were
288 performed by spiking known amounts of standards to blank QF filters. Then the spiked blank
289 filters were extracted and analyzed the same way as ambient collected samples. The average
290 recoveries of standard compounds are listed in supplemental information Table S5 and ranged
291 from 75.2 ± 5.6 to $129.4 \pm 4.2\%$. Isomers were identified for several compounds, no further
292 separation was conducted and combined total concentrations are reported in this study.

293

294 2.4 Source apportionment by Positive Matrix Factorization

295 Positive Matrix Factorization (PMF) was used to identify potential sources of compounds
296 measured at Coweeta. Here we use the PMF2 model (Paatero, 1998a, b) coupled with a bootstrap
297 technique (Hemann et al., 2009), which has been applied in a number of previous studies (Xie et
298 al., 2012, 2013, 2014,). Briefly, PMF resolves factor profiles and contributions from a series of
299 PM compositional data with an uncertainty-weighted least-squares fitting approach; the coupled
300 stationary bootstrap technique generates 1000 replicated data sets from the original data set and
301 each was analyzed with PMF. Normalized factor profiles were compared between the base case
302 solution and bootstrapped solutions, so as to generate a factor matching rate. The determination
303 of the factor number was based on the interpretability of different PMF solutions (3-6 factors)
304 and factor matching rate (>50%). Detailed data selection criteria are presented in supplemental
305 information.

306

307 3. Results and discussion

308 3.1 Meteorology, NO_x, and O₃

309 Statistics of atmospheric chemistry and meteorological measurements are summarized by
310 season in Table 1. In general, the sampling site was humid and cool, even in the summer, with
311 an average summer temperature of $\sim 21^\circ\text{C}$ and RH of 82%. During the fall, much lower
312 temperature ($\sim 12^\circ\text{C}$) and less humid conditions (RH=78%) were observed. NO_x concentrations

313 were generally less than 1ppb, which is considered typical for such a remote forest site removed
314 from major emission sources.

315 [O₃] (O₃ concentration) was generally low (Table 1) with seasonal averages of 15 ppb to
316 25 ppb. Historical seasonal [O₃] over the past 5 years (2011 to 2015) are shown in supplemental
317 information Figure S3. A spring maximum in [O₃] is typically observed at this site, with lower
318 concentrations during summer. Seasonal clustered back trajectories (Figure S4 in supplemental
319 information) suggest that during spring the Coweeta sampling site was under the influence from
320 air masses transported from Atlanta urban areas. In addition, a spring maximum [O₃] may be due
321 to higher chemical consumption of O₃ by reactive monoterpenes and sesquiterpenes emitted in
322 the forest during summer. With observed relatively moderate summer temperatures and
323 generally low [NO_x], the site also experiences frequent cloud cover in summer lowering the
324 intensity of solar radiation which may suppress ozone production relative to spring conditions.
325 Additionally, deposition of O₃ to the forest would be expected to peak during the summer, when
326 leaf area is greatest. O₃ correlates positively with NO_x in summer and fall but not spring,
327 indicating O₃ production might be relatively more VOC-limited in spring than the other seasons
328 in this region.

329

330 3.2 Bulk water soluble organic nitrogen and carbon

331 Water soluble bulk organic N (WSON) was estimated as the difference between WSTN
332 and the sum of the inorganic N species (NH₄⁺, NO₃⁻ and NO₂⁻). The measurement uncertainty of
333 WSON was estimated to be ~30% from error propagation of WSTN (2%), NH₄⁺ (1%), NO₃⁻ (1%)
334 and NO₂⁻ (1%). Nitrogen component contributions to WSTN are presented in Figure 1a, which
335 shows NH₄⁺ as the most abundant component, contributing 85±11% w/w to total WSTN mass.
336 Typical NH₄⁺ concentrations at the site were below 1.0 µg/m³(with an average of 0.32 µg/m³),
337 which is expected for such a remote site with no major local or regional NH₃ sources. The
338 oxidized inorganic N components (NO₃⁻ and NO₂⁻) accounted for less than 2% w/w of WSTN
339 measured. Such a small contribution of NO₃⁻ to inorganic N (typically <10% of inorganic N
340 (NO₃⁻+NH₄⁺)) in PM_{2.5} is consistent with long term CASTNET measurements at Coweeta. The
341 average contribution of WSON to WSTN over the entire study period was 14±11% w/w. This
342 fraction reached a maximum of ~18% w/w in the spring (average) and minimum of ~10% in the
343 fall (average), exhibiting pronounced seasonal variability. Within individual samples (Figure 1b),

344 values ranged from near zero to 45%. Our study wide average of 14% falls within the range of
345 measurements at North American forest sites, including Duke Forest, North Carolina (~33%, Lin
346 et al., 2010) and Rocky Mountain National Park (14-21%) (Benedict et al., 2012). Moreover, the
347 observed WSON contribution to WSTN in particles at Coweeta is consistent with a global
348 estimated range of 10-39% (Cape et al., 2011).

349 WSOC accounted for roughly $62 \pm 13\%$ of OC throughout the entire study period with no
350 significant seasonal variability. A time series of OC and WSOC along with temperature and
351 precipitation is presented in Figure 1c. On average, OC concentrations increased during warmer
352 spring and summer seasons and decreased when the temperature decreased in fall.
353 Concentrations of OC were positively correlated with temperature ($r=0.30$, $p<0.05$), presumably
354 in response to emissions of biogenic precursors and formation of secondary organic aerosols by
355 photooxidation. Spring and summer were generally moist and warm with frequent precipitation
356 (relative humidity presented in Table 1). Precipitation events corresponded to decreasing OC and
357 WSOC concentrations demonstrating the scavenging effect due to wet deposition.

358 Spearman rank correlation coefficients among measured species and meteorological
359 variables as well as other gas phase measurements are presented in Table 2 for each season
360 ($p<0.01$ for values in bold). As expected, NH_4^+ and SO_4^{2-} tracked well over each season ($r>0.9$,
361 $p<0.01$). NH_4^+ was mainly associated with SO_4^{2-} given the fact that NO_3^- and NO_2^- were
362 generally negligible compared to SO_4^{2-} . WSOC is often used as an SOA surrogate and accounts
363 for a significant portion (62% w/w) of OC during all sampling periods. WSOC correlated
364 strongly with OC over both summer and fall ($r>0.95$, $p<0.01$), but less so during spring ($r=0.74$,
365 $p<0.01$). WSOC also positively correlates with WSON over spring and fall ($r>0.75$, $p<0.01$) but
366 less so during summer ($r = 0.5$, $p > 0.01$). Note that both [WSOC] and [OC] are highest in the
367 summer, which likely indicates higher biogenic emissions and SOA formation. However, the
368 weak WSON-WSOC correlation suggests a variety of source contributions to WSON and WSOC
369 over the different seasons. [EC] was negligible over the entire study except a modest spike at the
370 end of October when wood burning was the most likely the source. It is also noted that a stronger
371 correlation of WSON with NH_4^+ than with NO_3^- was observed, which might suggest a key role
372 of reduced nitrogen in WSON formation (Cape et al., 2011; Jickells et al., 2013). Details of this
373 event are discussed in the subsequent sections.

374

375

376 3.3 Nitro-aromatics

377 Concentrations of nitro-aromatics, organosulfate/nitrooxy-organosulfate, and terpenoic
378 acids are summarized in Tables 3, S2, S3 and S4. A time series of compound class totals are
379 presented in Figure 2. Generally negligible concentrations of nitro-aromatics were observed
380 during spring and summer except for occasional spikes. However, higher concentrations of nitro-
381 aromatics were observed in the fall when moderate correlations were observed with levoglucosan
382 (Figure 3, $r \geq 0.5$, $p < 0.01$; see table SI 6 for correlation coefficients). A residential wood burning
383 contribution is likely given the lower temperatures observed during this season. Similar positive
384 correlations between nitro-aromatics and wood burning are also reported during the winter
385 season (Gaston et al., 2016; Kahnt et al., 2013; Kitanovski et al., 2012; Inuma et al., 2010,
386 2016). Smoke at the sampling site on October 19th and 21st coincided with firewood burning at
387 the main office of the Coweeta Hydrologic Laboratory, immediately adjacent to the sampling
388 location. Nitro-aromatics were relatively elevated, but no significant increase in organosulfates
389 or terpenoic acids were found from these fresh smoke events. In contrast, an example of an aged
390 biomass burning signal is illustrated on October 24th and 25th. Pronounced spikes of
391 nitrocatechol($C_6H_5NO_4$), methyl-nitrocatechol($C_7H_7NO_4$) and levoglucosan were observed
392 (Figure 3), along with elevated concentrations of organosulfates, OC and aged biogenic aerosol
393 tracers (terpenoic acids m/z 203 and 187 shown in Figure 4a, detailed discussion can be found in
394 the subsequent section). However, EC was only slightly higher. This event did not correspond to
395 local burning at Coweeta and was most likely associated with long range transport. Clustering of
396 backward trajectories (120hr duration for individual trajectories; 48 total trajectories covering the
397 two-day event) suggests that northeast Georgia (shown in supplemental information Figure S5) is
398 the most likely origin of the biomass burning event observed on October 24th and 25th.

399 Nitro-aromatics correlate with EC across the seasons; both are likely emitted from
400 biomass burning (Gaston et al., 2016; Inuma et al., 2010; Kahnt et al., 2013; Mohr et al., 2013).
401 Interestingly, light absorption at $\lambda = 365\text{nm}$ is highly correlated ($r = 0.80$, $p < 0.01$) with nitro-
402 aromatics in the fall when nitro-aromatic concentrations were elevated. In addition, NO_x
403 correlates inversely ($r = -0.72$, $p < 0.01$) with temperature in the fall. Lower fall temperatures in the
404 region may have resulted in frequent residential wood burning, which emits NO_x and light
405 absorbing BrC (eg. nitro-aromatics) (Liu et al., 2015; Mohr et al., 2013). Although nitro-

406 aromatics account for a minor fraction of OM, they could potentially contribute to 4% of light
407 absorption by BrC (Mohr et al., 2013). Overall, nitro-aromatics displayed relatively weak
408 correlation with WSON ($r < 0.65$) across all seasons; the extremely low concentrations observed
409 suggest a generally small contribution of nitro-aromatics to WSON at the sampling site, hence
410 the lack of strong correlation.

411

412 3.4 Organosulfates and nitrooxy-organosulfates

413 Organosulfate concentrations were highest in summer and lowest in fall (Table 3), contributing
414 3.9 and 1.0 % w/w of organic matter (OM, estimated by applying an OM/OC factor of 2) mass,
415 respectively, during these seasons. Organosulfate formation is an example of heterogeneous
416 chemistry involving uptake of reactive precursors on acidified sulfate aerosols requiring a
417 mixture of biogenic and anthropogenic emissions. The air masses at Coweeta are mainly from
418 the southwest and westerly directions in spring and summer, but during fall may become more
419 stagnant and slow moving during southwesterly conditions or shift to the northwest (see
420 clustered back trajectories are shown in Figure S4). Because Atlanta, GA is southwest of
421 Coweeta, southwesterly flow during spring and summer may be associated with long range
422 transport of urban pollutants and precursors, including sulfate and sulfuric acid, leading to
423 elevated organosulfate formation compared to fall when the prevailing wind direction changes.

424 Among all organosulfates identified, the isoprene derived organosulfate (m/z 215, 2-
425 methyltetrol derived), which is formed from isoprene derived epoxydiols (IEPOX) under low
426 NO_x conditions, was the most abundant; concentrations reached 167 ng/m^3 in summer. Similar
427 high concentrations were also reported in ambient samples collected at other sites in the
428 southeastern U.S. (Lin et al., 2013b; Worton et al., 2013). Of the six nitrooxy-organosulfates
429 identified, isoprene derived m/z 260 was most abundant, approximately 6-fold higher than
430 monoterpene derived m/z 294 nitrooxy-organosulfate.

431 A subset of possible organosulfates and nitrooxy-organosulfates produced from isoprene
432 and monoterpene oxidation exhibit strong correlations with distinctive SOA tracers (eg. markers
433 2-methylglyceric acid, C-5 alkene triols and methyltetrols for isoprene oxidation products; tracer
434 3-Hydroxyglutaric acid for pinene oxidation products) (see table SI 7). Lack of correlation
435 between nitrooxy-organosulfate m/z 294 and 3-hydroxyglutaric acid may indicate a nighttime
436 nitrate radical formation pathway rather than photochemical oxidation. Given that NO_x levels at

437 the rural Coweeta sampling site were typically less than 1ppb, photo-oxidation pathways
438 involving high [NO_x] to form nitrooxy-organosulfates are not likely. Nighttime nitrate radical
439 chemistry is the most likely formation mechanism under such conditions. In contrast to our
440 observations, He et al. (2014) report good correlations ($r>0.5$, $p<0.01$) of m/z 294 with 3-
441 hydroxyglutaric acid and higher daytime m/z 294 concentrations for summer samples collected
442 in Pearl River Delta, China, where a seasonal average NO_x level of 30 ppb was observed. The
443 authors suggested that the dominant m/z 294 formation pathway was through daytime
444 photochemistry rather than nighttime NO₃ chemistry. The extremely low NO_x levels at our study
445 site compared to that measured by He et al. may explain the opposite behavior in terms of m/z
446 294 formation mechanisms.

447 Organosulfates exhibited statistically significant correlations with WSON only in the
448 summer ($r=0.64$, $p<0.01$), which reflected the importance of N containing organosulfates or their
449 formation chemistry to WSON during summer compared to the other seasons. During this
450 season, nitrooxy-organosulfates accounted for ~2% of bulk WSON, on average. A strong
451 correlation may therefore not be expected.

452

453 3.5 Terpenoic acids

454 Terpenoic acids, which provide insight into the extent of biogenic compound oxidation
455 and atmospheric processing (i.e., aerosol aging), were the most abundant group of compounds
456 relative to nitro-aromatics and organosulfates. On average, terpenoic acids accounted for 6.5 to
457 8.7% w/w of OM in PM_{2.5}. The warmer spring and summer periods show higher production of
458 terpenoic acids compared to the cool and drier fall season. Higher emissions of biogenic VOC
459 precursors as well as higher solar radiation intensities during warm seasons, which drive
460 photochemistry, are factors contributing to observed seasonal variability.

461 The terpenoic acids correlate well with WSOC and OC (Table 2). This is expected as
462 terpenoic acids account for a substantial portion of OM at the site. Individual acids (except
463 compounds C₇H₁₀O₄ and C₉H₁₄O₄) exhibit strong correlations with the pinene derived SOA
464 tracer 3-hydroxyglutaric acid ($r>0.75$, $p<0.01$; correlation coefficients shown in the supplemental
465 information Table S8), indicating the presence of α -/ β -pinene oxidation products. The poor
466 correlations between acids C₇H₁₀O₄ (m/z 157) and C₉H₁₄O₄ (m/z 185) suggests the presence of

467 biogenic VOC precursors other than α -/ β -pinene, such as limonene and Δ^3 -carene (Gomez-
468 Gonzalez et al., 2012).

469 Recent chamber studies identified several terpenic acid structures also observed in
470 ambient aerosol samples, including 3-methyl-1,2,3-butanetricarboxylic acid (MBTCA, $C_8H_{12}O_6$,
471 m/z 203), 2-hydroxyterpenylic acid ($C_8H_{12}O_5$, m/z 187), terpenylic acid ($C_8H_{12}O_4$, m/z 171) and
472 diaterpenylic acid acetate (DTAA, $C_{10}H_{16}O_6$, m/z 231) (Claeys et al., 2009; Kahnt et al., 2014).
473 MBTCA and 2-hydroxyterpenylic acid have been identified as highly oxygenated, higher
474 generation α -pinene SOA markers, and observed in high abundance in ambient aerosols (Gomez-
475 Gonzalez et al., 2012; Kahnt et al., 2014; Muller et al., 2012; Szmigielski et al., 2007).
476 Additionally, terpenylic acid and DTAA are characterized as early photooxidation products from
477 α -pinene ozonolysis. Claeys et al. (2009) proposed further oxidation processes (aging) of
478 terpenylic acid involving OH radical chemistry to form 2-hydroxyterpenylic acid. Figure 4
479 provides a time series of the terpenic acids identified in this study. In general, 2-
480 hydroxyterpenylic acid was the most abundant species across the seasons. To assess the extent of
481 aging, concentration ratios of higher generation oxidation products ($C_8H_{12}O_6$, m/z 203 and
482 $C_8H_{12}O_5$, m/z 187) to early oxidation fresh SOA products ($C_8H_{12}O_4$, m/z 171 and $C_{10}H_{16}O_6$, m/z
483 231) are calculated. Estimated seasonal averages of these ratios are 3.98, 4.37 and 2.44 for
484 spring, summer and fall, respectively. Thus, during spring and summer, aerosols observed at the
485 site were more aged. Figure 4 shows the correlation of these ratios with temperature ($r=0.79$,
486 $p<0.001$) and solar radiation ($r=0.23$, $p<0.1$). A clear relationship between temperature and OH
487 radical initiated oxidation (aging) is evident. However, oxidation appears less dependent on solar
488 radiation at our sampling site. Similar higher contribution of these aged biogenic SOA tracers
489 was also reported under warm summer conditions characterized by high temperature and high
490 solar radiation (Claeys et al., 2012; Gomez-Gonzalez et al., 2012; Hamilton et al., 2013; Kahnt et
491 al., 2014). Based on the typical chemical lifetime of biogenic SOA by OH oxidation and the
492 precipitation frequency at Coweeta site, biogenic SOA collected at Coweeta probably had an
493 atmospheric lifetime of several days before depletion by oxidation processes and/or scavenging
494 by precipitation (Epstein et al., 2014).

495 Terpenic acids may also provide some insight into the formation mechanisms of
496 organosulfates. While organosulfate concentrations are highest during summer, correlations with
497 SO_4^{2-} are strongest during spring and fall and weakest during summer. Conversely,

498 organosulfates and terpenoic acids correlate strongly ($r=0.91$, $p<0.01$) during summer.
499 Terpenoic acids are either first or second generation oxidation products from gas phase
500 monoterpenes; particulate SO_4^{2-} abundance should not substantially influence the gas-particle
501 partitioning of terpenoic acids. The strong correlation between organosulfates and terpenoic
502 acids in summer suggests organosulfate formation is limited by monoterpene emissions rather
503 than SO_4^{2-} availability while in the spring and fall (especially fall), organosulfate production may
504 be more limited by SO_4^{2-} . Degree of particle neutralization, calculated as the molar ratio of NH_4^+
505 to the sum of SO_4^{2-} and NO_3^- , averaged 0.94, 0.98 and 0.94 for spring, summer and fall,
506 respectively. Neutralization being close to but less than unity implies that aerosols are slightly
507 acidic at the site. Chamber studies have illustrated that acidified SO_4^{2-} could enhance
508 heterogeneous reactions to form SOA from isoprene and monoterpenes (Inuma et al., 2009;
509 Surratt et al., 2007, 2010). Similar positive correlations observed at the Coweeta site were also
510 found between isoprene tracers including isoprene derived organosulfates and SO_4^{2-} by Lin et al.
511 (2013b) at a rural site in the southeastern U.S. However, in contrast to chamber experiments, this
512 study and other ambient field measurements have not provided clear evidence of acidity
513 enhancement of organosulfate formation (He et al., 2014; Lin et al., 2013b; Worton et al., 2011),
514 indicating possible differences in exact mechanisms and processing to form these organosulfates
515 under atmospheric conditions relative to chamber studies. Recent mechanistic modeling
516 simulations by Budisulistiorini et al., (2017) suggest that the role of sulfate on IEPOX-
517 organosulfates formation might be through surface area uptake of IEPOX and rate of particle
518 phase reaction.

519 Very good correlations between WSON and terpenoic acids were observed during summer
520 and fall ($r\geq 0.7$, $p<0.01$). Given the secondary nature of terpenoic acids, this finding may suggest
521 that WSON during these two seasons is associated with more aged air masses and perhaps
522 dominated by secondary organic components rather than primary emitted N containing
523 constituents such as pollens, fungi and bacteria (Elbert et al., 2007; Miyazaki et al., 2014).

524 3.6 Contribution of identified N containing species to WSTN and WSON

525 Nitro-aromatics and nitrooxy-organosulfates combined were estimated to account for as
526 much as 28% of WSON, which reflected the abundance and potential importance of these groups
527 of species to the atmospheric N deposition budget. Seasonal average ratios of identified WSON
528 to WSTN ranged from 1.0 to 4.4% with the highest recorded for fall (Table 4). Nitrooxy-

529 organosulfates dominated over nitro-aromatics as a source of organic nitrogen, contributing >
530 90% to identified WSON across seasons. However, during episodes of biomass burning, nitro-
531 aromatics contribute as much as 32% of identified WSON compounds. The ratio of WSON to
532 WSOC was estimated to be 0.05, 0.04 and 0.02 for spring, summer and fall, which implies
533 organic N being most enriched during spring, reflecting a spring maximum in seasonal emissions
534 of organic N from biological sources (e.g. pollens, spores, leave litter decomposition) combined
535 with smaller contributions from secondary atmospheric processes. The observed WSON/WSOC
536 ratios in this study were slightly lower than those reported for other forest sites (0.03-0.09) (Lin
537 et al., 2010; Miyazaki et al., 2014), which are not as remote and pristine as the forest site in this
538 study. Anthropogenic influences at the study sites described by Lin et al. (2010) and Miyazaki et
539 al. (2014) such as $[SO_4^{2-}]$ and $[NO_x]$ were ~ 5 times higher than those measured at the Coweeta
540 site. Concentration weighted average WSON/WSOC ratios for identified compounds (nitro-
541 aromatics, organosulfates/nitrooxy-organosulfates and terpenic acids) in this study were
542 estimated to be 0.003. This value is 10 times less than the overall WSON/WSOC ratio observed
543 at the site, which indicates existence of other higher N content species in the aerosols. Moreover,
544 the identified ON/WSON ratio was estimated to be 1.0, 2.0 and 4.4 for spring, summer and fall,
545 respectively. Such differences further suggest much more unidentified WSON compounds exist
546 in spring when organic N was most enriched from biological processes.

547

548 3.7 PMF analysis

549 PMF analysis was conducted to identify individual source contributions to total WSOC.
550 Factor profiles and time series of factor contributions are presented in figures 5 and 6. Listed in
551 order of percent contribution to WSOC, the five factors which were resolved include secondary
552 sulfate processing (35.3%), isoprene SOA (24.3%), WSON containing OM (20.0%), biomass
553 burning (15.1%) and monoterpene SOA (5.2%). Overall, these factors could explain $89 \pm 2\%$ of
554 observed WSOC ($r=0.88$, $p<0.0001$). The secondary sulfate profile contained a signature of high
555 SO_4^{2-} , which was most likely present as fine particulate $(NH_4)_2 SO_4$ and NH_4HSO_4 . Secondary
556 sulfate was the most important factor during spring, though was a significant contributor in
557 summer and fall as well. Isoprene SOA, which was identified based on isoprene derived
558 organosulfates and isoprene SOA markers, was the most important factor during summer. The
559 biomass burning factor, which exhibited a high portion of nitro-aromatic and levoglucosan

560 markers, dominated in the fall. This pattern agreed well with observed patterns of nitro-aromatic
561 compounds. Monoterpene SOA, which was resolved based on the composition of monoterpene
562 derived organosulfates, was overall a minor contributor with the exception of a few samples
563 during the fall intensive.

564 WSON containing OM contributed 20% to WSOC, overall, demonstrating a significant
565 association between organic N and C in PM_{2.5} at our study site. The WSON containing OM
566 source profile exhibited weak correlation with most measured species with the exception of
567 modest correlations with terpenoic acids. WSON containing OM contributed more to WSOC in
568 late spring and early summer, which was consistent with observed higher production of nitrooxy-
569 organosulfates during these sampling periods as well as terpenoic acids. The relationship with
570 terpenoic acids may reflect an association of WSON with more aged air masses. Because nitro-
571 aromatics and nitrooxy-organosulfates contribute only a small portion of WSON, on average, the
572 20% contribution of WSON containing OM to WSOC primarily reflects the contribution of
573 organic N present in bulk WSON but unspecified in this work.

574

575 4. Conclusions

576 Ambient PM_{2.5} collected at a temperate mountainous forest site were investigated on a bulk
577 chemical and a molecular level during spring, summer, and fall of 2015. Analyses focused on
578 speciation of nitro-aromatics associated with biomass burning, organosulfates produced from
579 biogenic SOA precursors, and terpenoic acids formed from monoterpene oxidation. Among these
580 three groups, terpenoic acids were estimated to be most abundant, contributing up to a seasonal
581 average of 8.7% of OM in PM_{2.5} during spring. Warm periods in spring and summer exhibited
582 highest production of terpenoic acids, when SOA correspondingly showed a higher degree of
583 aging. Relative abundance of aged biogenic SOA tracers (MBTCA and 2-hydroxyterpenylic
584 acid), which reflect the degree of organic aerosol aging, showed a strong correlation with
585 temperature. Such a relationship might indicate temperature dependence of OH radical initiated
586 oxidation steps or aging in the formation of higher generation oxidation products.

587 Organosulfates showed a peak in summer and lowest concentrations during fall,
588 contributing averages of 3.9 and 1.0 % of OM mass, respectively, during these seasons. Isoprene
589 derived organosulfate (m/z 215, 2-methyltetrol derived), formed from isoprene derived
590 epoxydiols (IEPOX) under low NO_x conditions, was the most abundant identified organosulfate

591 (up to 167 ng/m³ in summer). This observation is consistent with observations of low NO_x
592 levels (< 1ppb on average) at our study site. Nighttime nitrate radical chemistry is most likely the
593 dominant formation mechanism for nitrooxy-organosulfates measured at this remote site with
594 background level NO_x.

595 Nitro-aromatics were most abundant at our study site during the fall (up to 0.01% of OM
596 mass). Moderate correlations were observed between nitro-aromatics and the biomass burning
597 marker levoglucosan, indicating a common origin. Nitro-aromatics also correlated well with EC
598 across seasons. Highest concentrations of nitro-aromatics, specifically nitrocatechol and methyl-
599 nitrocatechol, were associated with aged biomass burning plumes as indicated by
600 correspondingly high concentrations of terpenoic acids.

601 Bulk measurements determined that WSOC accounted for 62±13% of OC throughout the
602 entire study period without significant seasonal variability. PMF analysis indicated that a
603 significant portion of this organic carbon was associated with a resolved factor of WSON
604 containing OM. As a component of total nitrogen in PM_{2.5}, largest contributions of WSON to
605 WSTN were observed in spring (~ 18% w/w) and lowest in the fall (~10% w/w). On average,
606 identified nitro-aromatic and nitrooxy-organosulfate compounds accounted for a small fraction
607 of WSON, ranging from ~ 1% in spring to ~ 4% in fall, though were observed to contribute as
608 much as 28% w/w of WSON in individual samples which were impacted by local biomass
609 burning. Of the organic N compounds speciated in this study, nitrooxy-organosulfates dominated
610 over nitro-aromatics as a source of organic nitrogen, contributing > 90% to WSON across
611 seasons. As a component of WSON, nitro-aromatics were most important during episodes of
612 biomass burning, when their contribution to identified and total WSON was as much as 32% and
613 3%, respectively. Concentration weighted average WSON/WSOC ratios for compounds
614 identified in this study were estimated to be 0.003. This number is an order of magnitude lower
615 than the overall WSON/WSOC ratio observed, indicating a predominance of other
616 uncharacterized N species. Other N containing substituents of WSON could include amino
617 acids, amines, urea and N-heterocyclic compounds as well as substances of biological origin
618 such as spores, pollens and bacteria (Cape et al., 2011; Neff et al., 2002a). Ratios of WSON to
619 WSOC indicate organic C being most enriched by organic N during spring, perhaps reflecting a
620 spring maximum in seasonal emissions of organic N from biological sources combined with
621 smaller contributions from secondary atmospheric processes (e.g., nitrooxy-organosulfates).

622 Although nitro-aromatics and nitrooxy-organosulfates contribute a relatively small
623 fraction of organic N in PM_{2.5} at our study site, our observations shed light on this complex but
624 largely unknown portion of the atmospheric N budget. Our results provide further understanding
625 of the patterns and composition of SOA in a remote mountain environment previously
626 uncharacterized. Similar to our results, other studies generally find that individual groups of
627 organic N compounds (e.g., amines, amino acids, urea) cannot explain the majority of bulk
628 WSON, (Cape et al., 2011; Day et al., 2010; Place et al., 2017; Samy et al., 2013), which
629 globally accounts for ~25% of total N in rainfall (Cape et al., 2011; Jickells et al., 2013). As
630 methodological advances allow for greater speciation of this large pool of atmospheric N, future
631 work should emphasize analysis of both primary and secondary forms of organic N in individual
632 samples, in addition to bulk analyses, so that a more complete picture of organic N composition
633 may be developed for specific atmospheric chemical and meteorological conditions.
634 Additionally, as progress is made in better characterizing the composition and sources of
635 atmospheric organic N, the ecological and atmospheric science communities must work together
636 to develop a better understanding of the role of atmospheric organic N in ecosystem N cycling.

637

638 **Supplemental Information available**

639

640 **Acknowledgements**

641

642 We would like to acknowledge Pamela Barfield, Ryan Daly, Aleksandra Djurkovic, David
643 Kirchgessner, John Offenberg, Bakul Patel and Bill Preston for laboratory and field support. We
644 also would like to thank Joshua G. Hemann and Michael P. Hannigan for the PMF source codes
645 and Christopher Oishi, Patsy Clinton and Chuck Marshall for assistance with meteorological data
646 sets. We would like to thank the U.S. Forest Service, Southern Research Station for the
647 opportunity to conduct this study at the Coweeta Hydrologic Laboratory and for the contribution
648 of meteorological data used in our analysis. We also thank internal EPA reviewers Chris Geron
649 and Havala Pye for their comments and suggestions. The views expressed in this article are those
650 of the authors and do not necessarily represent the views or policies of the U.S. EPA. Mention
651 of trade names does not constitute endorsement or recommendation of a commercial product by
652 U.S. EPA.

653

654

655 **References**

- 656 Altieri, K.E., Turpin, B.J., and Seitzinger S.P., 2009. Composition of dissolved organic nitrogen
657 in continental precipitation investigated by Ultra-High Resolution FT-ICR Mass Spectrometry.
658 *Environmental Science and Technology* 43, 6950-6955.
659
- 660 Altieri, K.E., Hastings, M.G., Peters, A.J., Sigman, D.M., 2012. Molecular characterization of
661 water soluble organic nitrogen in marine rainwater by ultra-high resolution electrospray
662 ionization mass spectrometry. *Atmospheric Chemistry and Physics* 12. 3557-3571.
663
- 664 Benedict, K.B., 2012. Observations of atmospheric reactive nitrogen species and nitrogen
665 deposition in the Rocky Mountains. Dissertation, Colorado State University.
666 <https://dspace.library.colostate.edu/handle/10217/71545>
- 667 Birch, M. E. and Cary, R. A.: Elemental carbon-based method for monitoring occupational
668 exposures to particulate diesel exhaust, *Aerosol Science and Technology*, 25, 221–241, 1996.
669
- 670 Bobbink, R., Hornung M., and Roelofs, J.M., 1998. The effects of air-borne nitrogen pollutants
671 on species diversity in natural and semi-natural European vegetation. *Journal of Ecology* 86,
672 717-738.
673
- 674 Bolstad, P.V., Swank, W., Vose, J., 1998. Predicting Southern Appalachian overstory vegetation
675 with digital terrain data. *Landscape Ecology* 13, 271-283.
676
- 677 Bragazza, L., Freeman, C., Jones, T., Rydin, H., Limpens, J., Fenner, N., Ellis, T., Gerdol, R.,
678 Hajek, M., Iacumin, P., Kutnar, L., Tahvanainen, T., and Toberman, H., 2006. Atmospheric
679 nitrogen deposition promotes carbon loss from peat bogs. *Proceedings of the national academy*
680 *of Science* 103, 19386-19389.
681
- 682 Budisulistiorini, S.H., Nenes, A., Carlton, A.G., Surratt, J.D., McNeill, V.F., Pye, H.O.T., 2017.
683 Simulating aqueous-phase isoprene-epoxydiol(IEPOX) secondary organic aerosol production
684 during the 2013 Southern Oxidation and Aerosol Study(SOAS). *Environmental Science and*
685 *Technology* 51, 5026-5034.
686
- 687 Cape, J.N., Cornell, S.E., Jickells, T.D., Nemitz, E., 2011. Organic nitrogen in the atmosphere-
688 Where does it come from? A review of sources and methods. *Atmospheric Research* 102, 30-48.
689
- 690 Chan, M.N., Surratt, J.D., Claeys, M., Edgerton, E.S., Tanner, R.L., Shaw, S.L., Zheng, M.,
691 Knipping, E.M., Eddingsaas, N.C., Wennberg, P.O., Seinfeld, J.H., 2010. Characterization and
692 quantification of isoprene-derived epoxydiols in ambient aerosol in the Southeastern United
693 States. *Environmental Science and Technology* 44, 4590-4596.
694
- 695 Chen, Y., Bond, T.C., 2010. Light absorption by organic carbon from wood combustion.
696 *Atmospheric Chemistry and Physics* 10, 1773-1787.
697
- 698 Cheng, Y., He, K.-b., Du, Z.-y., Engling, G., Liu, J.-m., Ma, Y.-l., Zheng, M., Weber, R.J., 2016.

699 The characteristics of brown carbon aerosol during winter in Beijing. *Atmospheric Environment*
700 127, 355-364.

701

702 Claeys, M., Graham, B., Vas, G., Wang, W., Vermeylen, R., Pashynska, V., Cafmeyer, J.,
703 Guyon, P., Andreae, M.O., Artaxo, P., Maenhaut, W., 2004. Formation of secondary organic
704 aerosols through photooxidation of isoprene. *Science* 303, 1173-1176.

705

706 Claeys, M., Szmigielski, R., Kourchev, I., Van Der Veken, P., Vermeylen, R., Maenhaut, W.,
707 Jaoui, M., Kleindienst, T.E., Lewandowski, M., Offenberg, J.H., Edney, E.O., 2007.
708 Hydroxycarboxylic acids: Markers for secondary organic aerosol from the photooxidation of
709 α -pinene. *Environmental Science and Technology* 41, 1628-1634.

710

711 Claeys, M., Iinuma, Y., Szmigielski, R., Surratt, J.D., Blockhuys, F., Van Alsenoy, C., Boge, O.,
712 Sierau, B., Gomez-Gonzalez, Y., Vermeylen, R., Van Der Veken, P., Shahgholi, M., Chan,
713 A.W.H., Herrmann, H., Seinfeld, J.H., Maenhaut, W., 2009. Terpenylic acid and related
714 compounds from the oxidation of α -pinene: Implications for new particle formation and growth
715 above forests. *Environmental Science and Technology* 43, 6976-6982.

716

717 Claeys, M.; Vermeylen, R.; Yasmeeen, F.; Gómez-González, Y.; Chi, X. G.; Maenhaut, W.;
718 Mészáros, T.; Salma, I., 2012. Chemical characterisation of humic-like substances from urban,
719 rural and tropical biomass burning environments using liquid chromatography with UV/vis
720 photodiode array detection and electrospray ionization mass spectrometry. *Environmental*
721 *Chemistry* 9, 273–284.

722

723 Darer, A.I., Cole-Filipiak, N.C., O'Connor, A.E., Elrod, M.J., 2011. Formation and stability of
724 atmospherically relevant isoprene-derived organosulfates and organonitrates. *Environmental*
725 *Science and Technology* 45, 1895-1902.

726

727 Day, D. A., Liu, S., Russell, L. M. and Ziemann, P. J., 2010. Organonitrate group concentrations
728 in submicron particles with high nitrate and organic fractions in coastal southern California.
729 *Atmospheric Environment* 44, 1970–1979.

730

731 Doney, S.C., Mahowald, N., Lima, I., Feely, R.A., Mackenzie, F.T., Lamarque, J-F., and Rasch,
732 P.J., 2007. Impact of anthropogenic atmospheric nitrogen and sulfur deposition on ocean
733 acidification and the inorganic carbon system. *Proceedings of the national academy of Science*
734 104, 14580-14585.

735

736 Elbert, W., Taylor, P.E., Andreae, M.O., Poschl, U., 2007. Contribution of fungi to primary
737 biogenic aerosols in the atmosphere: wet and dry deposited spores, carbohydrates, and
738 inorganic ions. *Atmospheric Chemistry and Physics* 7, 4569-4588.

739

740 Epstein, S.A., Blair, S.L., Nizkorodov, S.A., 2014. Direct photolysis of α -pinene ozonolysis
741 secondary organic aerosol: effect on particle mass and peroxide content. *Environmental Science*
742 *and Technology* 48, 11251-11258.

743

744 Fehsenfeld, F.C., Dickerson, R.R., Hubler, G., Luke, W.T., Nunnermacker, L.J., Williams, E.J.,

744 Roberts, J.M., Calvert, J.G., Curran, C.M., Delany, A.C., Eubank, C.S., Fahey, D.W., Fried, A.,
745 Grandrud, B.W., Langford, A.O., Murphy, P.C., Norton, R.B., Pickering, K.E., Ridley, B.A.,
746 1987. A ground-based intercomparison of NO, NO_x and NO_y measurement techniques. *Journal*
747 *of Geophysical Research* 92, 14710-14722.

748
749 Gaston, C.J., Lopez-Hifiker, F.D., Whybrew, L.E., Hadley, O., McNair, F., Gao, H., Jaffe, D.A.,
750 Thornton, J.A., 2016. Online molecular characterization of fine particulate matter in Port Angeles,
751 WA: Evidence for a major impact from residential wood smoke. *Atmospheric Environment* 138,
752 99-107.

753
754 Gomez-Gonzalez, Y., Surratt, J. D., Cuyckens, F., Szmigielski, R., Vermeylen, R., Jaoui, M.,
755 Lewandowski, M., Offenberg, J. H., Kleindienst, T. E., Edney, E. O., Blockhuys, F., Van
756 Alsenoy, C., Maenhaut, W., and Claeys, M., 2008. Characterization of organosulfates from the
757 photooxidation of isoprene and unsaturated fatty acids in ambient aerosol using liquid
758 chromatography/(-) electrospray ionization mass spectrometry, *Journal of Mass Spectrometry*,
759 43, 371–382.

760
761 Gomez-Gonzalez, Y., Wang, W., Vermeylen, R., Chi, X., Neiryneck, J., Janssens, I.A., Maenhaut,
762 W., Claeys, M., 2012. Chemical characterization of atmospheric aerosols during a 2007 summer
763 field campaign at Brasschaat, Belgium: sources and source processes of biogenic secondary
764 organic aerosol. *Atmospheric Chemistry and Physics* 12, 125-138.

765
766 Gonzalez Benitez, J.M., Cape, J.N., Heal, M.R., van Dijk, N., Vidal Diez, A., 2009. Atmospheric
767 nitrogen deposition in south-east Scotland: Quantification of the organic nitrogen fraction in wet,
768 dry and bulk deposition. *Atmospheric Environment* 43, 4087-4094.

769
770 Hamilton, J.F., Alfarra, M.R., Robinson, N., Ward, M.W., Lewis, A.C., McFiggans, G.B., Coe,
771 H., Allan, D., 2013. Linking biogenic hydrocarbons to biogenic aerosol in the Borneo rainforest.
772 *Atmospheric Chemistry and Physics* 13, 11295-11305.

773
774 He, Q-F., Ding, X., Wang, X-M., Yu, J.Z., Fu, X-X., Liu, T-Y., Zhang, Z., Xue, J., Chen, D-H.,
775 Zhong, L-J., Donadue, N.M., 2014. Organosulfates from pinene and isoprene over the Pearl
776 River Delta, South China: Seasonal variation and implication in formation mechanisms.
777 *Environmental Science and Technology* 48, 9236-9245.

778
779 Hecobian, A., Zhang, X., Zheng, M., Frank, N., Edgerton, E.S., Weber, R.J., 2010. Water
780 Soluble Organic Aerosol material and the light-absorption characteristics of aqueous extracts
781 measured over the Southeastern United States. *Atmospheric Chemistry and Physics* 10, 5965-
782 5977.

783
784 Hemann, J.G., Brinkman, G.L., Dutton, S.J., Hannigan, M.P., Milford, J.B., Miller, S.L., 2009.
785 Assessing positive matrix factorization model fit: a new method to estimate uncertainty and bias
786 in factor contributions at the measurement time scale. *Atmospheric Chemistry and Physics* 9,
787 497-513.

788
789 Hungate, B.A., Dukes, J.S., Shaw, M.R., Luo, Y., and Field C.B., 2003. Nitrogen and Climate
790 Change. *Science* 302, 1512-1513.

791 Iinuma, Y., Boge, O., Kahnt, A., Herrmann, H., 2009. Laboratory chamber studies on the
792 formation of organosulfates from reactive uptake of monoterpene oxides. *Physical Chemistry*
793 *Chemical Physics* 11, 7985-7997.
794

795 Iinuma, Y., Boge, O., Grafe, R., Herrmann, H., 2010. Methyl-nitrocatechols : atmospheric
796 tracers compounds for biomass burning secondary organic aerosols. *Environmental Science and*
797 *Technology* 44, 8453-8459.
798

799 Iinuma, Y., Keywood, M., Herrmann, H., 2016. Characterization of primary and secondary
800 organic aerosols in Melbourne airshed: The influence of biogenic emissions, wood smoke and
801 bushfires. *Atmospheric Environment* 130, 54-63.
802

803 Jickells, T., Baker, A.R., Cape, J.N., Cornell, S.E., Nemitz, E., 2013. The cycling of organic
804 nitrogen through the atmosphere. *Philosophical Transactions of the Royal Society B*
805 368:20130115.
806

807 Kahnt, A., Behrouzi, S., Vermeylen, R., Safi Shalamzari, M., Vercauteren, J., Roekens, E.,
808 Claeys, M., Maenhaut, W., 2013. One-year study of nitro-organic compounds and their relation
809 to wood burning in PM10 aerosol from a rural site in Belgium. *Atmospheric Environment* 81,
810 561-568.
811

812 Kahnt, A., Iinuma, Y., Blockhuys, F., Mutzel, A., Vermeylen, R., Kleindienst, T.E., Jaoui, M.,
813 Offenberg, J.H., Lewandowski, M., Boge, O., Herrmann, H., Maenhaut, W., Claeys, M., 2014.
814 2-Hydroxyterpenylic acid: an oxygenated marker compound for α -pinene secondary organic
815 aerosol ambient fine aerosol. *Environmental Science and Technology* 48, 4901-4908.
816

817 Kanakidou, M., Duce, R.A., Prospero, J.M., Baker, A.R., Benitez-Nelson, C., Dentener, F.J.,
818 Hunter, K.A., Liss, P.S., Mahowald, N., Okin, G.S., Sarin, M., Tsigaridis, K., Uematsu, M.,
819 Zamora, L.M., Zhu, T., 2012. Atmospheric fluxes of organic N and P to the global ocean. *Global*
820 *Biogeochemical Cycles* 26, GB3026, doi:10.1029/2011GB004277.
821

822 Keene, W.C., Montag, J.A., Maben, J.R., Southwell, M., Leonard, J., Church, T.M., Moody, J.L.,
823 Galloway, J.N., 2002. Organic nitrogen in precipitation over Eastern North America.
824 *Atmospheric Environment* 36, 4529-4540.
825

826 Kitanovski, Z., Grgic, I., Vermeylen, R., Claeys, M., Maenhaut, W., 2012. Liquid
827 chromatography tandem mass spectrometry method for characterization of monoaromatic nitro-
828 compounds in atmospheric particulate matter. *Journal of Chromatography A* 1268, 35-43.
829

830 Kleindienst, T. E., Jaoui, M., Lewandowski, M., Offenberg, J.H., Lewis, C.W., Bhave, P.V.,
831 Edney, E.O., 2007. Estimates of the contributions of biogenic and anthropogenic hydrocarbons
832 to secondary organic aerosol at a southeastern US location. *Atmospheric Environment* 41, 8288-
833 8300.
834

835 Lin, M., Walker, J., Geron, C., Khlystov, A., 2010. Organic nitrogen in PM2.5 aerosol at a forest
836 site in the Southeast US. *Atmospheric Chemistry and Physics* 10, 2145-2157.

837
838 Lin, Y-H., Zhang, H., Pye, H.O.T., Zhang, Z., Marth, W.J., Park, S., Arashiro, M., Cui, T.,
839 Hapsari Budisulistiorini, S., Sexton, K.G., Vizuete, W., Xie, Y., Luecken, D.J., Piletic, I.R.,
840 Edney, E.O., Bartolotti, L.J., Gold, A., Surratt, J.D., 2013a. Epoxide as a precursor to secondary
841 organic aerosol formation from isoprene photooxidation in the presence of nitrogen oxides.
842 *Proceedings of the National Academy of Science* 110, 6718-6723.
843
844 Lin, Y-H., Knipping, E.M., Edgerton, E.S., Shaw, S.L., Surratt, J.D., 2013b. Investigating the
845 influences of SO₂ and NH₃ levels on isoprene-derived secondary organic aerosol formation
846 using conditional sampling approaches. *Atmospheric Chemistry and Physics* 13, 8457-8470.
847
848 Liu, J., Bergin, M., Guo, H., King, L., Kotra, N., Edgerton, E., Weber, R.J., 2013. Size-resolved
849 measurements of brown carbon in water and methanol extracts and estimates of their
850 contribution to ambient fine-particle light absorption. *Atmospheric Chemistry and Physics* 13,
851 12389-12404.
852
853 Liu, J., Scheuer, E., Dibb, J., Diskin, G.S., Ziemba, L.D., Thornhill, K.I., Anderson, B.E.,
854 Wisthaler, A., Mikoviny, T., Devi, J.J., Bergin, M., Perring, A.E., Markovic, M.Z., Scheartz,
855 J.P., Campuzano-Jost, P., Day, D.A., Jimenez, J.L., Weber, R.J., 2015. Brown carbon aerosol in
856 the North American continental troposphere: sources, abundance, and radiative forcing.
857 *Atmospheric Chemistry and Physics* 15, 7841-7858.
858
859 Lohse, K.A., Hope, D., Sponseller, R., Allen, J.O., Grimm, N.B., 2008. Atmospheric deposition
860 of carbon and nutrients across an arid metropolitan area. *Science of the Total Environment* 402,
861 95-105.
862
863 Magnani, F., Mencuccini, M., Borghetti, M., Berbigier, P., Berninger, F., Delzon, S., Grelle, A.,
864 Hari, P., Jarvis, P.G., Kolari, P., Kowalski, A.S., Lankreijer, H., Law, B.E., Lindroth, A.,
865 Loustau, D., Manca, G., Moncrieff, J.B., Rayment, M., Tedeschi, V., Valentini, R., Grace, J.,
866 2007. The human footprint in the carbon cycle of temperate and boreal forests. *Nature* 447, 848-
867 850.
868
869 Meade, L.E., Riva, M., Blomberg, M.Z., Brock, A.K., Qualters, E.M., Siejack, R.A.,
870 Ramakrishnan, K., Surratt, J.D., Kautzman, K.E., 2016. Seasonal variation of fine particulate
871 organosulfates derived from biogenic and anthropogenic hydrocarbons in the mid-Atlantic
872 United States. *Atmospheric Environment* 145, 405-414.
873
874 Miniati, C.F., Laseter, S.H., Swank, W.T., Swift, L.W. Jr., 2015. Daily air temperature, relative
875 humidity, vapor pressure, PPF, wind speed and direction for climate stations at the Coweeta
876 Hydrologic Lab, North Carolina. Fort Collins, CO: Forest Service Research Data Archive.
877 Updated 28 February 2017. <https://doi.org/10.2737/RDS-2015-0042>
878
879
880 Miyazaki, Y., Fu, P., Ono, K., Tachibana, E., Kawamura, K., 2014. Seasonal cycles of water-
881 soluble organic nitrogen aerosols in a deciduous broadleaf forest in northern Japan. *Journal of*
882 *Geophysical Research: Atmospheres* 119, 1440-1454.

883
884 Mohr, C., Lopez-Hilfiker, F.D., Zotter, P., Prevot, A.S.H., Xu, L., Ng, N.L., Herndon, S.C.,
885 Williams, L.R., Franklin, J.P., Zahniser, M.S., Worsnop, D.R., Knighton, W.B., Aiken, A.C.,
886 Gorkowski, K.J., Dubey, M.K., Allan, J.D., Thornton, J.A., 2013. Contribution of nitrated
887 phenols to wood burning brown carbon light absorption in Detling, United Kingdom during
888 winter time. *Environmental Science and Technology* 47, 6316-6324.
889
890 Muller, L.; Reinnig, M.-C.; Naumann, K. H.; Saathoff, H.; Mentel, T. F.; Donahue, N. M.;
891 Hoffmann, T., 2012. Formation of 3-methyl-1,2,3- butanetricarboxylic acid via gas phase
892 oxidation of pinonic acid – a mass spectrometric study of SOA aging. *Atmospheric Chemistry*
893 *and Physics* 12, 1483–1496.
894
895 Neff, J.C., Holland, E.A., Dentener, F.J., Mcdowell, W.H., Russell, K.M., 2002a. The origin,
896 composition and rates of organic nitrogen depiction: A missing piece of the nitrogen cycle?
897 *Biogeochemistry* 57/58, 99-136.
898
899 Neff, J.C., Townsend, A.R., Gleixner, G., Lehman, S.J., Turnbull, J., Bowman, W., 2002b.
900 Variable effects of nitrogen additions on the stability and turnover of soil carbon. *Nature* 419,
901 915-917.
902
903 Oishi, A.C., Miniati, C.F., Novick, K.A., Brantley, S.T., Vose, J.M., Walker, J.T., 2017. Warmer
904 temperatures reduce net carbon uptake, but do not affect water use, in a mature southern
905 Appalachian forest. *Agricultural and Forest Meteorology*. In press.
906
907 Ollinger, S.V., Aber, J.D., Reich, P.B., Freuder, R.J., 2002. Interactive effects of nitrogen
908 deposition, tropospheric ozone, elevated CO₂ and land use history on the carbon dynamics of
909 northern hardwood forests. *Global Change Biology* 8, 545-562.
910
911 Paatero, P. User's Guide for Positive Matrix Factorization Program PMF2 and PMF3, Part 1:
912 Tutorial. University of Helsinki: Helsinki, Finland, 1998a.
913
914 Paatero, P. User's Guide for Positive Matrix Factorization Program PMF2 and PMF3, Part 2:
915 Reference. University of Helsinki: Helsinki, Finland, 1998b.
916
917 Place, B. K., Quilty, A. T., Di Lorenzo, R. A., Ziegler, S. E., and VandenBoer, T. C. ,2017.
918 Quantitation of 11 alkylamines in atmospheric samples: separating structural isomers by ion
919 chromatography, *Atmospheric Measurement Techniques* 10, 1061–1078.
920
921 Pregitzer, K.S., Burton, A.J., Zak, D.R., and Talhelm, A.F., 2008. Simulated chronic nitrogen
922 deposition increases carbon storage in Northern Temperate forests. *Global Change Biology* 14,
923 142-153.
924
925 Samy, S., Robinson, J., Rumsey, I.C., Walker, J.T., Hays, M.D., 2013. Speciation and trends of
926 organic nitrogen in southeastern U.S. fine particulate matter (PM_{2.5}). *Journal of Geophysical*
927 *Research: Atmospheres* 118, 1996-2006.
928
929 Shalamzari, M.S., Vermeylen, R., Blockhuys, F., Kleindienst, T.E., Lewandowski, M.,

930 Szmigielski, R., Rudzinski, K.J., Spolnik, G., Danikiewicz, W., Maenhaut, W., Claeys, M., 2016.
931 Characterization of polar organosulfates in secondary organic aerosol from the unsaturated
932 aldehydes 2-E-pentenal, 2-E-hexenal, and 3-Z-hexenal. *Atmospheric Chemistry and Physics* 16,
933 7135-7148.

934
935 Simkin, S.M., Allen, E.B., Bowman, W.D., Clark, C.M., Belnap, J., Brooks, M.L., Cade, B.S.,
936 Collins, S.L., Geiser, L.H., Gilliam, F.S., Jovan, S.E., Pardo, L.H., Schulz, B.K., Stevens, C.J.,
937 Suding, K.N., Throop, H.L., and Waller, D.M., 2016. Conditional vulnerability of plant diversity
938 to atmospheric nitrogen deposition across the United States. *Proceedings of the national*
939 *academy of Science* 113, 4086-4091.

940
941 Surratt, J. D., Murphy, S.M., Kroll, J.H., Ng, N.L., Hildebrandt, L., Sorooshian, A., Szmigielski,
942 R., Vermeylen, R., Maenhaut, W., Claeys, M., Flagan, R.C., Seinfeld, J.H., 2006. Chemical
943 composition of secondary organic aerosol formed from the photooxidation of isoprene. *Journal*
944 *of Physical Chemistry A* 110, 9665-9690.

945
946 Surratt, J.D., Kroll, J.H., Kleindienst, T.E., Edney, E.O., Claeys, M., Sorooshian, A., Ng, N.L.,
947 Offenberg, J.H., Lewandowski, M., Jaoui, M., Flagan, R.C., Seinfeld, J.H., 2007. Evidence for
948 organosulfates in secondary organic aerosol. *Environmental Science and Technology* 41, 517-
949 527.

950
951 Surratt, J.D., Gomez-Gonzalez, Y., Chan, A.W.H., Vermeylen, R., Shahgholi, M., Kleindienst,
952 T.E., Edney, E.O., Offenberg, J.H., Lewandowski, M., Jaoui, M., Maenhaut, W., Claeys, M.,
953 Flagan, R.C., Seinfeld, J.H., 2008. Organosulfate formation in biogenic organic aerosol. *Journal*
954 *of physical chemistry A* 112, 8345-8378.

955
956 Surratt, J.D., Chan, A.W.H., Eddingsaas, N.C., Chan, M.N., Loza, C.L., Kwan, A.J., Hersey,
957 S.P., Flagan, R.C., Wennberg, P.O., Seinfeld, J.H., 2010. Reactive intermediates revealed in
958 secondary organic aerosol formation from isoprene. *Proceedings of the National Academy of*
959 *Science* 107, 6640-6645.

960
961 Swank, W.T. and D.A. Crossley, Jr..1988. Introduction and site description. In *Forest Hydrology*
962 *and Ecology at Coweeta*. 169 pp. Edited by W.T. Swank and D.A. Crossley, Jr. Springer-Verlag,
963 Berlin.

964
965 Swift, L.W..Jr., G.B. Cunningham and J.E. Douglass. 1988. *Climatology and Hydrology*. In
966 *Forest Hydrology and Ecology at Coweeta*. 469 pp. Edited by W.T. Swank and D.A. Crossley,
967 Jr. Springer-Verlag. Berlin

968
969 Szmigielski, R.; Surratt, J. D.; Gómez-González, Y.; Van der Veken, P.; Kourtchev, I.;
970 Vermeylen, R.; Blockhuys, F.; Jaoui, M.; Kleindienst, T. E.; Lewandowski, M.; Offenberg, J. H.;
971 Edney, E. O.; Seinfeld, J. H.; Maenhaut, W.; Claeys, M., 2007. 3-methyl-1,2,3-
972 butanetricarboxylic acid: An atmospheric tracer for terpene secondary organic aerosol.
973 *Geophysical Research Letter* 34, L24811.

974

975 U.S. EPA, 2017. U.S. Environmental Protection Agency Clean Air Markets Division,
976 Clean Air Status and Trends Network (CASTNET). Hourly ozone and meteorology.
977 Available at www.epa.gov/castnet. Date accessed: 01/15/2017.
978

979 Walker, J.T., Dombek, T.L., Green, L.A., Gartman, N., Lehmann, C.M.B., 2012. Stability of
980 organic nitrogen in NADP wet deposition samples. *Atmospheric Environment* 60, 573-582.
981

982 Williams, E.J.; Baumann, K.; Roberts, J.M.; Bertman, S.B.; Norton, R.B.; Fehsenfeld, F.C.;
983 Springston, S.R.; Nunnermacker, L.G.; Newman, L.; Olszyna, K; Meagher, J.; Hartsell, B.;
984 Edgerton, E.; Perason, J.R.; Rodgers, M.O., 1998. Intercomparison of ground-based NO_y
985 measurements techniques. *Journal of Geophysical Research: Atmospheres* 103, 22261-22280.
986

987 Worton, D. R., Goldstein, A. H., Farmer, D. K., Docherty, K. S., Jimenez, J. L., Gilman, J. B.,
988 Kuster, W. C., de Gouw, J., Williams, B. J., Kreisberg, N. M., Hering, S. V., Bench, G., McKay,
989 M., Kristensen, K., Glasius, M., Surratt, J. D., Seinfeld, J. H., 2011. Origins and composition of
990 fine atmospheric carbonaceous aerosol in the Sierra Nevada Mountains, California. *Atmospheric
991 Chemistry and Physics* 11, 10219–10241.
992

993 Worton, D.R., Surratt, J.D., LaFranchi, B.W., Chan, A.W.H., Zhao, Y., Weber, R.J., Park, J-H.,
994 Gilman, J.B., de Gouw, J., Park, C., Schade, G., Beaver, M., St. Clair, J.M., Crounse, J.,
995 Wennberg, P., Wolfe, G.M., Harrold, S., Thornton, J.A., Farmer, D.K., Docherty, K.S., Cubison,
996 M.J.M., Jimenez, J-L., Frossard, A.A., Russell, L.M., Kristensen, K., Glasius, M., Mao, J., Ren,
997 X., Brune, W., Browne, E.C., Pusede, S.E., Cohen, R.C., Seinfeld, J.H., Goldstein, A.H., 2013.
998 Observational insights into aerosol formation from isoprene. *Environmental Science and
999 Technology* 47, 11403-11413.
1000

1001 Xie, M., Hannigan, M.P., Dutton, S.J., Milford, J.B., Hemann, J.G., Miller, S.L., Schauer, J.J.,
1002 Peel, J.L., Vedal, S., 2012. Positive matrix factorization of PM_{2.5}: Comparison and implications
1003 of using different speciation data sets. *Environmental Science & Technology* 46, 11962-11970
1004

1005 Xie, M., Barsanti, K.C., Hannigan, M.P., Dutton, S.J., Vedal, S., 2013. Positive matrix
1006 factorization of PM_{2.5} - eliminating the effects of gas/particle partitioning of semivolatile
1007 organic compounds. *Atmospheric Chemistry and Physics* 13, 7381-7393.
1008

1009 Xie, M., Hannigan, M.P., Barsanti, K.C., 2014. Impact of Gas/Particle Partitioning of
1010 Semivolatile Organic Compounds on Source Apportionment with Positive Matrix Factorization.
1011 *Environmental Science & Technology* 48, 9053-9060.
1012

1013 Zellweger, C., Ammann, M., Buchmann, B., Hofer, P., Lugauer, M., Ruttimann, R., Streit, N.,
1014 Weingartner, E., Baltensperger, U., 2000. Summertime NO_y speciation at the Jungfrauoch,
1015 3580m above sea level, Switzerland. *Journal of Geophysical Research* 105, 6655-6667.
1016

1017 Zhang, Y., Song, L., Liu, X.J., Li, W.Q., Lu, S.H., Zheng, L.X., Bai, Z.C., Cai, G.Y., Zhang,
1018 F.S., 2012. Atmospheric organic nitrogen deposition in China. *Atmospheric Environment* 46,
1019 195-204.

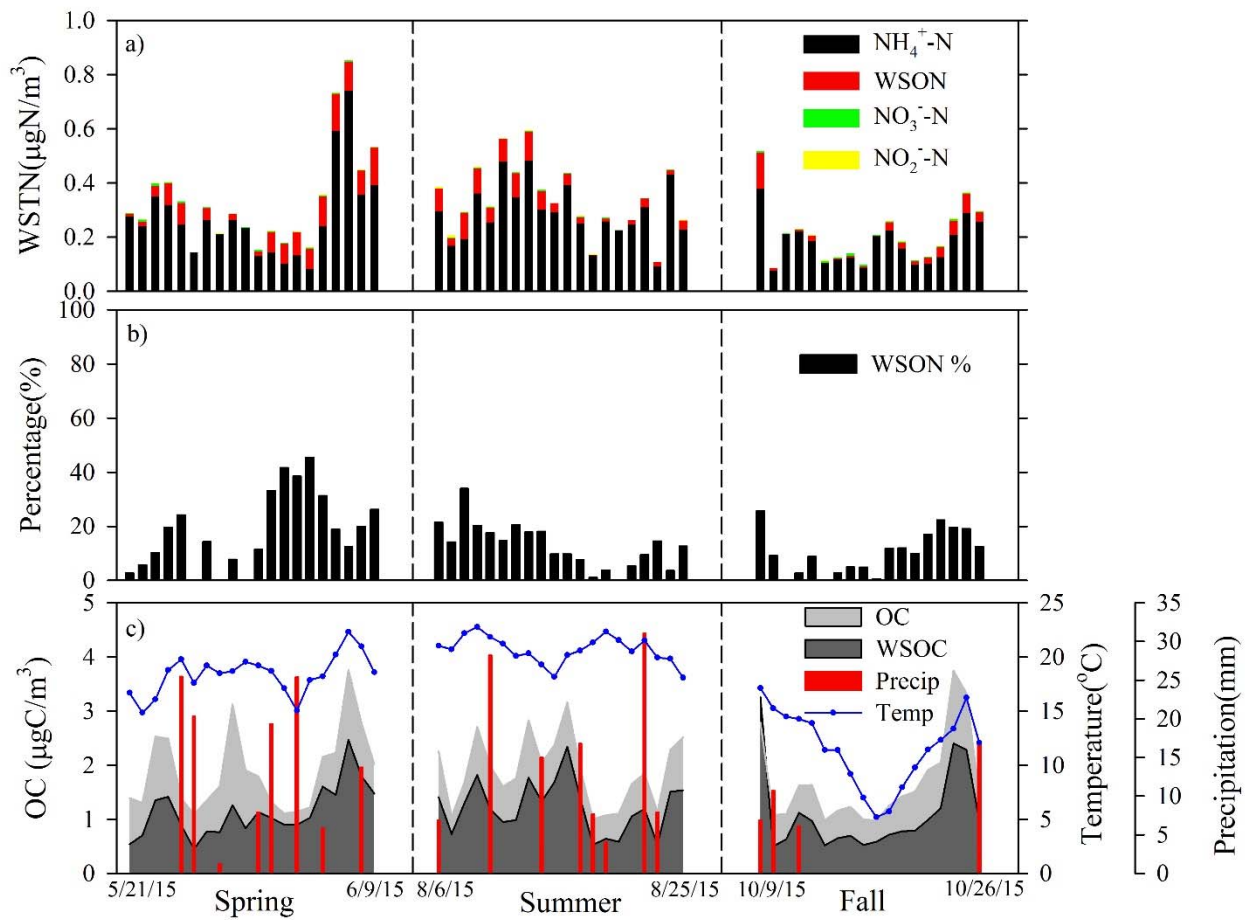


Figure 1. a) Individual concentrations of nitrogen components to WSTN (NH_4^+ , NO_3^- , NO_2^- and WSON); b) Percent contribution of WSON to WSTN; c) Time series of OC, WSOC, temperature and precipitation. Start and end dates of each intensive sampling periods are shown.

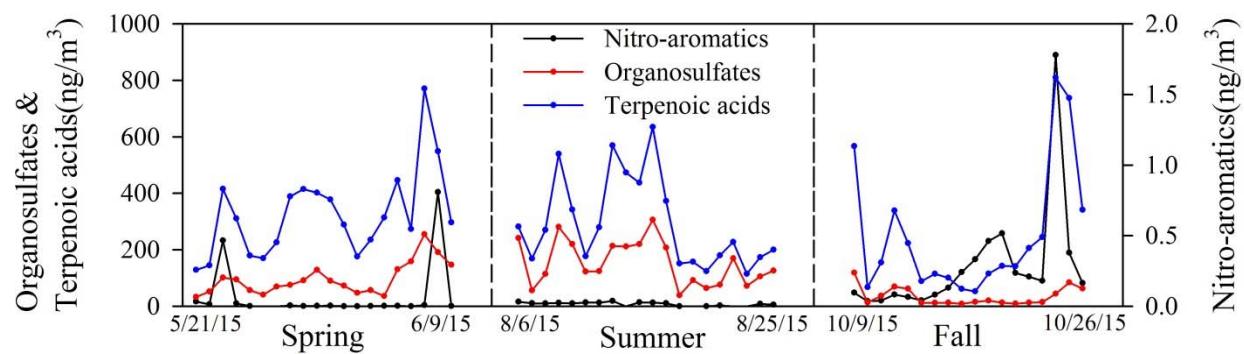


Figure 2. Time series of summed compound group concentrations of nitro-aromatics, organosulfates and terpenoic acids.

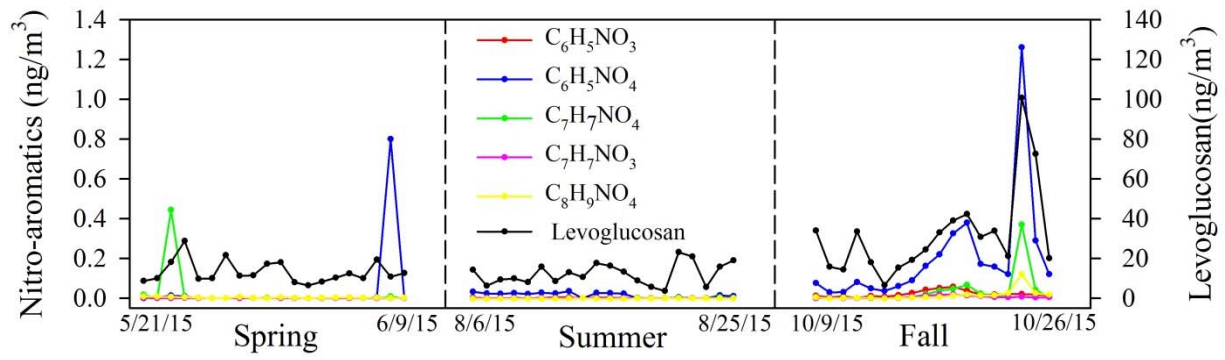


Figure 3. Time series of individual nitro-aromatics compounds as well as levoglucosan.

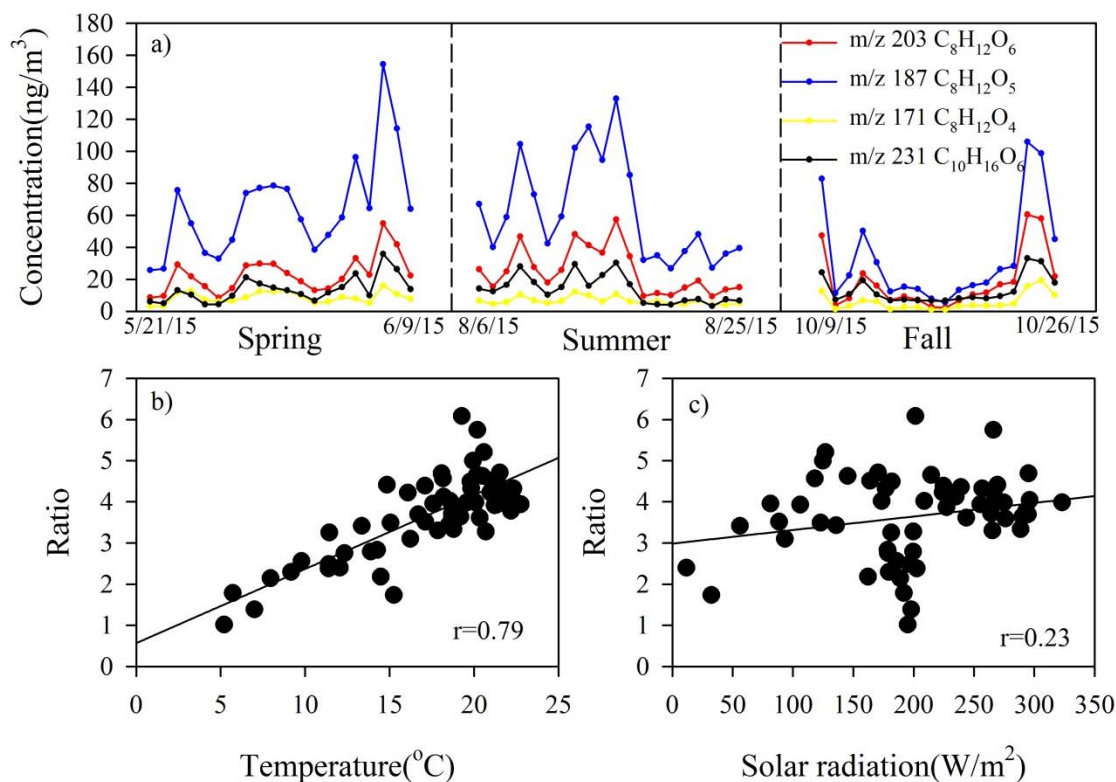


Figure 4. a) Time series of these four identified terpenoic acids(3-methyl-1,2,3-butaneetricarboxylic acid(MBTCA, C₈H₁₂O₆, m/z 203), 2-hydroxyterpenylic acid(C₈H₁₂O₅, m/z 187), terpenylic acid(C₈H₁₂O₄, m/z 171) and Diaterpenylic acid acetate(DTAA, C₁₀H₁₆O₆,m/z 231)); b) correlation of concentration ratios of higher generation oxidation products(C₈H₁₂O₆, m/z 203 and C₈H₁₂O₅, m/z 187) to early oxidation fresh SOA products(C₈H₁₂O₄, m/z 171 and C₁₀H₁₆O₆,m/z 231) with temperature and ; c) with solar radiation.

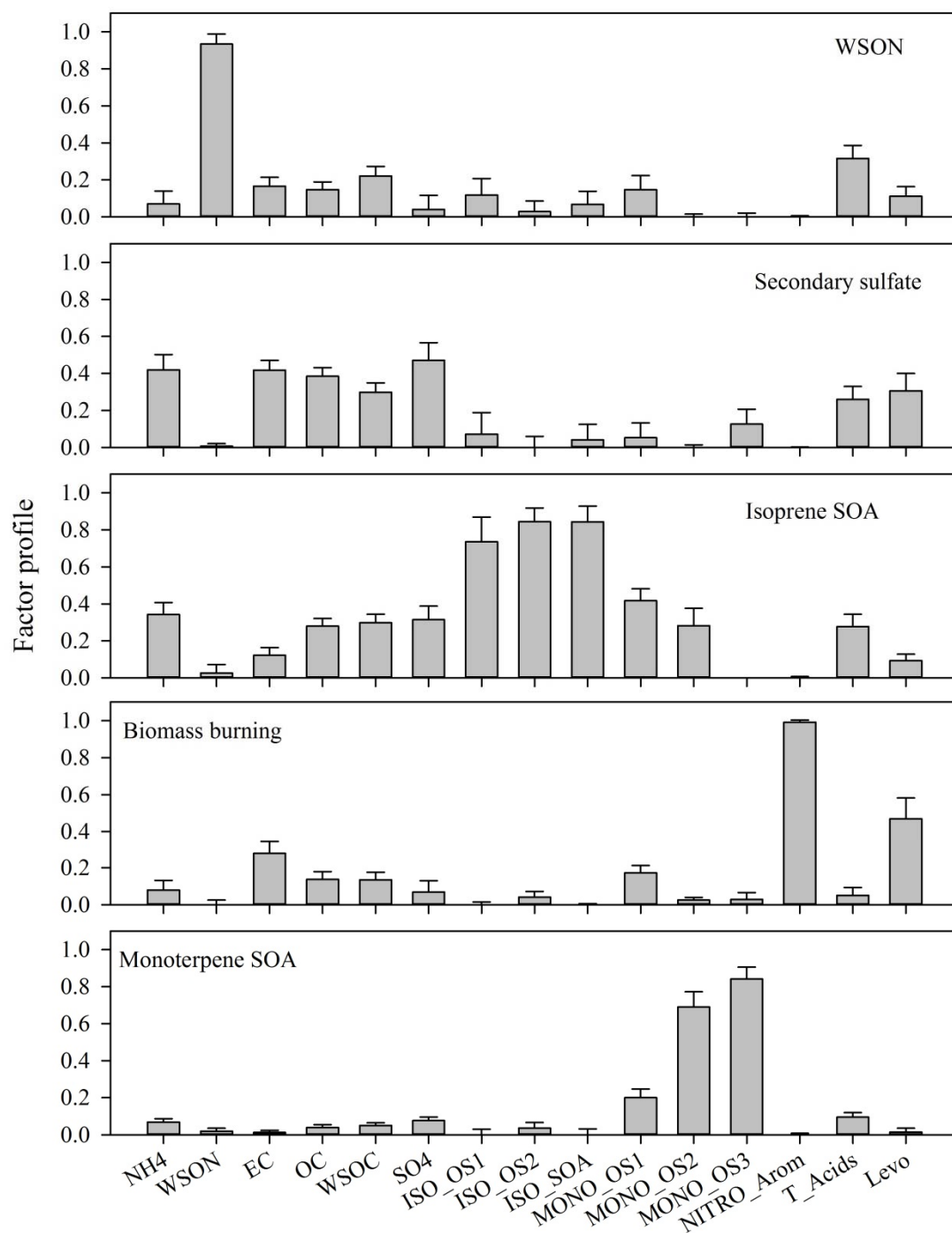


Figure 5. Normalized factor profiles (error bar represents one standard deviation).

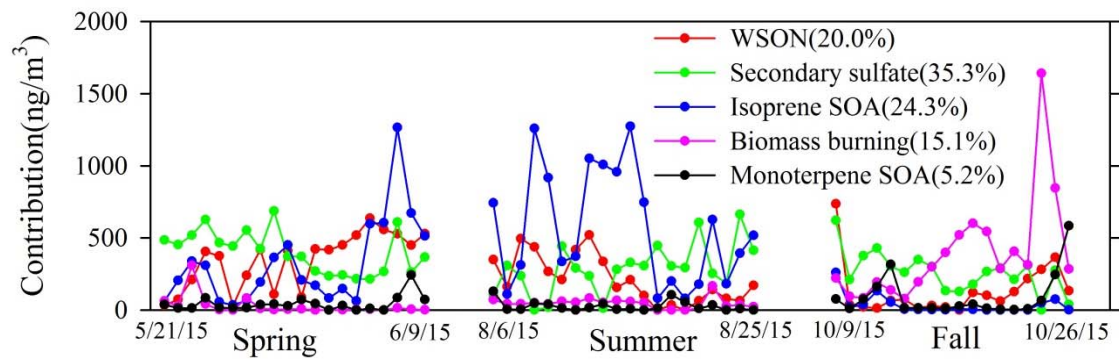


Figure 6. Time series of factor contributions to WSOC (mean factor contribution shown in brackets).

Table 1. Summary of particulate and gaseous species measured at Coweeta sampling site in 2015.

(μg/m ³)	Spring				Summer				Fall			
	mean	median	min	max	mean	median	min	max	mean	median	min	max
OM (OC*2)	3.77	3.41	2.18	7.52	3.80	3.79	2.00	6.32	3.36	2.85	1.96	7.49
EC	0.05	0.05	0.03	0.10	0.05	0.05	0.02	0.08	0.07	0.07	0.03	3.75
WSOC	1.14	1.03	0.45	2.47	1.22	1.24	0.53	2.34	1.09	0.78	0.50	3.25
WSTN	0.33	0.29	0.14	0.86	0.34	0.32	0.11	0.59	0.21	0.20	0.08	0.52
WSON	0.06	0.07	ND	0.14	0.05	0.03	ND	0.11	0.03	0.02	ND	0.13
NH ₄ ⁺ -N	0.27	0.24	0.08	0.74	0.29	0.28	0.09	0.48	0.18	0.17	0.08	0.38
NO ₃ ⁻ -N	0.00	0.00	ND	0.01	0.00	0.00	ND	0.01	0.00	0.00	ND	0.01
NO ₂ ⁻ -N	0.00	0.00	ND	0.00	0.00	0.00	ND	0.01	0.00	0.00	ND	0.00
SO ₄ ²⁻	0.99	0.93	0.26	2.44	1.01	0.95	0.31	1.85	0.63	0.58	0.30	1.33
O ₃ (ppb)	25.1	21.6	13.9	46.1	15.8	15.8	9.0	22.8	19.4	20.5	11.1	26.9
NOx(ppb)	0.75	0.79	0.45	1.03	0.54	0.58	0.24	0.91	0.65	0.68	0.43	0.89
Temp(°C)	18.4	18.6	14.8	22.3	20.7	20.6	18.1	22.8	11.6	11.7	5.2	17.1
RH%	81.7	84.9	61.0	94.8	82.1	83.1	71.9	88.5	77.7	74.9	65.1	92.0
Radiation	235	265	81	296	205	201	106	323	151	180	12	203

Table 3. Seasonal statistics of measured groups of compounds.

(ng/m ³)	Spring				Summer				Fall			
	mean	median	min	max	mean	median	min	max	mean	median	min	max
Nitro-aromatics	0.07	0.00	ND	0.81	0.02	0.02	ND	0.04	0.28	0.17	0.04	1.78
Organo-sulfates ¹	96.77	83.05	33.07	255.17	153.36	125.41	38.93	306.66	34.69	15.27	0.17	118.68
Terpenoic acids	325.62	304.05	128.68	771.16	294.01	249.19	115.08	634.99	250.66	148.91	52.94	809.46
% of OM ²												
%Nitro-aromatics	0.00	0.00	ND	0.02	0.00	0.00	ND	0.00	0.01	0.01	0.00	0.02
%Organo-sulfates	2.47	2.42	1.19	3.64	3.87	3.80	1.95	5.56	0.98	0.63	0.31	2.21
% Terpenoic acids	8.65	8.29	4.62	12.88	7.50	7.77	3.80	11.64	6.48	5.21	2.70	12.00

¹ including nitrooxy-organosulfates; ²Fraction of each group of identified compounds (combined total) to organic matter

Table 4. Ratios of identified nitrogen containing compounds (nitro-aromatics and nitrooxy-organosulfates) to WSON.

(ngN/m ³)	Spring				Summer				Fall			
	mean	median	min	max	mean	median	min	max	mean	median	min	max
WSON	59	74	ND	140	46	33	ND	105	25	15	ND	133
Identified ON	0.48	0.36	0.1	1.75	0.65	0.53	0.12	1.83	0.46	0.26	0.07	1.70
Identified ON/WSON %	1.02	0.64	ND	3.09	2.04	1.71	ND	7.84	4.37	1.50	ND	27.90